Fish and Shellfish Immunology 94 (2019) 373–380

Contents lists available at ScienceDirect

Fish and Shellfish Immunology

journal homepage: www.elsevier.com/locate/fsi

Full length article

Identification of a novel RIG-I isoform and its truncating variant in Japanese eel, *Anguilla japonica*

B. Huang[a,b,1], Z.X. Wang[a,1], C. Zhang[a], S.W. Zhai[a], Y.S. Han[c], W.S. Huang[a,b,*], P. Nie[d,**]

[a] Fisheries College, Jimei University, Xiamen, 361021, China
[b] Engineering Research Center of the Modern Technology for Eel Industry, Ministry of Education, PR China
[c] Institute of Fisheries Science, National Taiwan University, Taipei, 10617, Taiwan
[d] School of Marine Science and Engineering, Qingdao Agricultural University, Qingdao, Shandong Province, 266109, China

ARTICLE INFO

Keywords:
RIG-I
Splicing variant
Expression
Cellular distribution
IFN promoter inducibility
Japanese eel
Anguilla japonica

ABSTRACT

Retinoic acid-inducible gene-I (RIG-I) is a cytoplasmic viral RNA sensor that triggers the production of type I interferons (IFNs) and proinflammatory cytokines during viral infection. RIG-I gene has been identified previously in Japanese eel, *Anguilla japonica*. In the present study, we have characterized a novel isoform of RIG-I (designated as AjRIG-Ib) and its truncated variant (AjRIG-Ibv). The AjRIG-Ib encodes 940 amino acids (aa) consisting of two N-terminal caspase activation and recruitment domains (CARDs), a DEX(D/H) box RNA helicase domain, and a C-terminal regulatory domain (CTD). The AjRIG-Ibv encodes a protein of 843 aa, that shares similar structural organization with AjRIG-Ib, but lacking CTD. The gene expression analyses showed that AjRIG-Ib and AjRIG-Ibv were detectable in all tissues/organs examined, and AjRIG-Ib was the predominant form. The mRNA level of AjRIG-Ibv was upregulated rapidly at 8 h after the Poly I:C injection, and the significant increase of AjRIG-Ib was observed at 16 and 24 h post-injection (hpi). Laser confocal microscopy showed that AjRIG-Ib and AjRIG-Ibv were both located in cytoplasm. In addition, the overexpression of AjRIG-Ib or AjRIG-Ibv led to the increased activity of IFN promoter in transient transfection assay. Taken together, our results indicated that AjRIG-Ib and AjRIG-Ibv may play cooperative or somewhat complementary roles in coordinating the antiviral response in fish.

1. Introduction

Innate immune system is the front line for host defense against pathogenic microorganisms [1]. In the innate immune system, pattern recognition receptors (PPRs) are responsible for recognizing conserved microbial features that are called pathogen associated molecular patterns (PAMPs), including bacterial cell wall components, microbial nucleic acids, and certain highly conserved proteins [2,3]. Retinoic acid inducible gene I (RIG-I)-like receptors are a family of DExD/H box RNA helicases that function as viral RNA sensors in antiviral defense program [4]. This family consists of three homologous proteins with two of them, RIG-I and melanoma differentiation associated gene 5 (MDA5), recognizing complementary sets of viral dsRNA ligands, leading to the production of IFN as well as proinflammatory cytokines and chemokines [5,6]. The another member, laboratory of genetics and physiology 2 (LGP2), has been implicated in regulating RIG-I and MDA5 signaling pathways [7,8]. RIG-I was originally described in pig as RNA helicase (denoted RHIV-1) induced upon infection with porcine reproductive and respiratory syndrome virus (PPRSV) [9]. Subsequent studies have shown that RIG-I recognizes a wide variety of RNA viruses, for example, members of the Paramyxoviridae (such as Sendai virus, Newcastle disease virus, etc.), Rhabdoviridae (Vesicular stomatitis virus and Rabies virus) [10–12], Orthomyxoviridae (Influenza A and B) [13,14], Filoviridae (Ebola) [15], and Arenaviridae (Lassa and Lymphocytic choriomeningitis virus) [15,16]. Upon ligand binding, RIG-I undergoes a series of conformational changes, switching from the auto-repressed resting state to the activated conformation, which allows RIG-I to interact with the scaffold protein, mitochondrial antiviral signaling protein (MAVS; also known as VISA, IPS-1 or Cardif) on the mitochondrial membrane [17]. This interaction induces MAVS aggregation and subsequent signal propagation, which leads to the activation of nuclear factor κB (NF-κB) and/or interferon regulatory factors (IRFs),

* Corresponding author. Fisheries College, Jimei University, Xiamen, 361021, China.
** Corresponding author.
E-mail addresses: wshuang@jmu.edu.cn (W.S. Huang), pinnie@ihb.ac.cn (P. Nie).
[1] These two authors contributed equally to this work.

https://doi.org/10.1016/j.fsi.2019.09.037
Received 30 June 2019; Received in revised form 7 September 2019; Accepted 14 September 2019
Available online 15 September 2019

Table 1
Primers used in this study.

Primer	Sequence (5′–3′)	Application
AjRIG-Ib-F	ATGTACGAGACGGAGAAGG	ORF amplification
Aj-RIG-Ib-R	TTAAAAGGGCTTTATATCCG	
AjRIG-Ib-pc3.1/Flag-F	GCGATATCGCCACCATGTACGAGACGGAGAAG	Eukaryotic expression plasmid construction
AjRIG-Ib-pc3.1/Flag-R	CGGGATCCAAAGGGCTTTATATCCG	
AjRIG-Ibv-pc3.1/Flag-R	CGGGATCCTACCTCCTGTCCCACC	
qAjRIG-Ib-F	CTATGCAAGCTAAGATTGACATC	Real-time PCR
qAjRIG-Ib-R	GTGATGTGACCCCTCCTGT	
qAjRIG-Ibv-F	GGACAGGAGGTATGATTCTTCTTG	
qAjRIG-Ibv-R	CGTTCAACTTGACTGGTGCAG	
qAjELF1-α-F	GCCAGCAGCAATATGTCCTG	
qAjELF1-α-R	GGTACAGTTCCAATACCTCCA	
AjIFN2-pro-F	CTAGCTAGCTTGTAGCCTACCTGTACACGTT	Luciferase plasmid construction
AjIFN2-pro-R	CCCAAGCTTTCTCGCGTCCATGGCTTA	
AjIFN4-pro-F	CTAGCTAGCCTTACAACTTAAACTTCCCTCAAT	
AjIFN4-pro-R	CCCAAGCTTAGGGAGGGTTAAGCACAGTC	

promoting interferon (IFN) or pro-inflammatory cytokine production [18,19].

Accumulated evidences have shown that fish possess unique features in the components of innate immune recognition, including some gene family expansion or contraction [20]. For example, there are 10 numbers of Toll like receptor (TLR) reported from human (termed TLR1 to TLR10), whereas at least 17 types of TLRs have been identified in teleost fish, with several of them being fish-specific [21]. RIG-I, which shows an evolutionary continuity from amphibians to mammals, has only been identified from a few species of fish, including Atlantic salmon (*Salmo salar*), crucian carp (*Carassius auratus*), grass carp (*Ctenopharyngodon idella*), channel catfish (*Ictalurus punctatus*), common carp (*Cyprinus carpio*), zebrafish (*Danio rerio*) and Japanese eel (*Anguilla japonica*) [22–30]. Although there is no any direct evidence regarding the RNA-binding activity of teleost RIG-I, the overexpression of RIG-I in fish cells can lead to a strong induction of IFNs and interferon stimulated genes (ISGs). Moreover, teleost RIG-I also exhibited antiviral activity against spring viremia of carp virus (SVCV), viral hemorrhagic septicemia virus (VHSV) and grass carp reovirus (GCRV), suggesting a functional conservation of RIG-I among teleost and mammals [23,25,28]. Further, it was reported that alternative splicing occurs in fish RIG-I gene. Four different transcripts of RIG-I, termed RIG-Ia, b, c, d, have been reported in zebrafish [31]. RIG-Ib, which resembles mammalian RIG-I in many aspects, such as gene structure, can induce type I IFN promoter activity and antiviral state in fish cell line. RIG-Ia, containing 38 amino acids insertion, lacks the ability to induce IFN promoter activity, being unable to protect cells during SVCV infection, whereas the function of latter RIG-I variants (RIG-Ic and RIG-Id) still remain enigmatic [28,31].

In this study, a novel isoform of RIG-I (namely AjRIG-Ib) and its splice variant (AjRIG-Ibv) that lacks the last domain, a C-terminal regulatory domain (CTD), were identified and characterized from the Japanese eel. Their intracellular localization and temporal expression profiles in response to Poly I:C challenge were investigated, and their activation effect on eel type I IFN promoters were examined using luciferase reporter assay.

2. Materials and methods

2.1. Fish and Poly I:C stimulation

Japanese eels of approximately 100 g were purchased from a local fish farm and maintained in the laboratory at 28 °C with a re-circulating water system. Prior to experiments, fish were acclimatized to laboratory conditions for 2 weeks with the permission from College of Fisheries, Jimei University. Tissues/organs, including liver, intestine, head kidney, middle kidney, skin, spleen and gill, collected from ten intact healthy fish were used for tissue distribution analysis. For challenge experiment, twenty-four eels were each injected intraperitoneally with 0.2 mg of Poly I:C (Sigma) dissolved in sterile phosphate-buffered saline (PBS, pH 7.4), whereas another twenty-four control eels were injected with the same volume of PBS. The head kidney, spleen, liver, skin, gill and intestine were collected at 8, 16, 24 and 72 h post injection (hpi) for RNA isolation.

2.2. RNA extraction and cDNA synthesis

Total RNA was extracted from each sample using Trizol (Invitrogen Corp) according to the manufacturer's instruction. RNA samples were treated with DNase I to remove genomic DNA contamination using gDNA Eraser Kit (Takara). The RNA concentration and quality were determined by Nanodrop 2000 spectrophotometry and agarose gel electrophoresis (Thermo Scientific, USA). In order to obtain the open reading frame, 2 μg total RNA from spleen was reverse-transcribed into cDNA using SMART™ RACE cDNA Amplification Kit (Takara) with oligo dT primer, according to the manufacturer' s instruction. For expression analysis, 2 μg of total RNA from each sampled tissues/organs was reverse-transcribed into cDNA by random primers using GoScript™ Reverse Transcription System (Promega).

2.3. RIG-I gene cloning and bioinformatic analysis

The zebrafish RIG-I coding sequence (GenBank accession No. AGN48009.1) was used as query for BLAST search against the Japanese eel genome database retrieved from GenBank (https://www.ncbi.nlm.nih.gov/). Gene specific primers were designed based on BLASTx results (https://blast.ncbi.nlm.nih.gov/Blast.cgi) (Table 1). PCR products of the expected size were purified with EZNAO Gel Extraction Kit (Omega, Bio-Tek), and ligated in a pMD19-T vector (Promega) before being transformed into *Escherichia coli* strain DH5a. The positive clones were fully sequenced using M13 forward and reverse primers targeting the amplification of cloning site in the vector.

The deduced amino acid sequences were analyzed using the ExPASy translate tool (https://web.expasy.org/translate/). The protein domains were predicted with CD-search (https://www.ncbi.nlm.nih.gov/Structure/cdd/wrpsb.cgi). The conserved motifs were analyzed through InterProscan (https://www.ebi.ac.uk/interpro/search/sequence-search). Multiple alignments were performed on ClustalW program. Sequence similarity and identity calculations were performed using the MatGAT program [32].

Phylogenetic trees were constructed based on the amino acid sequences listed in Table 2. NJ tree was made by MEGA7.0 with standard setting and 10 000 bootstrap replicates. ML tree, presented in the Supplementary Data, was constructed by RAxML software with

Table 2
RIG-I like receptors used for sequence alignment and phylogenetic tree construction.

Protein	Species	Database accession number
RIG-I	*Homo sapiens*	ENSG00000107201
RIG-I	*Mus musculus*	ENSMUSG00000040296
RIG-I	*Ornithorhynchus anatinus*	ENSOANG00000012131
RIG-I	*Pelodiscus sinensis*	ENSPSIG00000013490
RIG-I	*Anolis carolinensis*	ENSACAG00000001354
RIG-I	*Latimeria chalumnae*	ENSLACG00000000411
RIG-I	*Scleropages formosus*	ENSSFOG00015017386
RIG-Ia	*Lepisosteus oculatus*	ENSLOCG00000006504
RIG-Ib	*Lepisosteus oculatus*	ENSLOCG00000013422
RIG-I	*Eptatretus burgeri*	ENSEBUG00000014150
RIG-I	*Petromyzon marinus*	ENSPMAG00000009697
RIG-I	*Pygocentrus nattereri*	ENSPNAG00000002347
RIG-I	*Astyanax mexicanus*	ENSAMXG00000015795
RIG-I	*Paramormyrops kingsleyae*	ENSPKIG00000017174
RIG-I	*Esox lucius*	ENSELUG00000005444
RIG-I	*Anguilla japonica*	KT156978*
RIG-Ib	*Anguilla japonica*	MK838769*
RIG-Ibv	*Anguilla japonica*	MK838770*
RIG-Ia	*Danio rerio*	AGN48008.1*
RIG-Ib	*Danio rerio*	AGN48009.1*
RIG-Ic	*Danio rerio*	AEN04472.1*
RIG-Id	*Danio rerio*	AGN48011.1*
RIG-I	*Ctenopharyngodon idella*	AGH30714.1*
RIG-I	*Ictalurus punctatus*	AFS34609.1*
RIG-I	*Salmo salar*	CAX48607.2*
RIG-I	*Cyprinus carpio*	ADZ55452.1*
RIG-I	*Carassius auratus*	AEN04472.1*
LGP2	*Homo sapiens*	ENSG00000108771
LGP2	*Mus musculus*	ENSMUSG00000017830
LGP2	*Gallus gallus*	ENSGALG00000023821
LGP2	*Anolis carolinensis*	ENSACAG00000012501
LGP2	*Latimeria chalumnae*	ENSLACG00000011208
MDA5	*Homo sapiens*	ENSG00000115267
MDA5	*Mus musculus*	ENSMUSG00000026896
MDA5	*Gallus gallus*	ENSGALG00000041192
MDA5	*Anolis carolinensis*	ENSACAG00000014017
MDA5	*Latimeria chalumnae*	ENSLACG00000011448

* Sequence were retrieved from NCBI database.

JTT + gamma model suggested as the best model by ProtTest3 [33,34]. Node support was assessed with 100 bootstrapping replicates.

2.4. Analysis of gene expression

Real-time PCR was performed with a Roche Light-Cycler480 Real-time PCR system (Roche, Switzerland), using iQ™ SYBR® Green SuperMix (Bio-Rad). The reaction mixtures were incubated for 5 min at 94 °C, followed by 40 cycles of 5 s at 94 °C, 20 s at 60 °C, and 30 s at 72 °C. To determine the efficiency of the PCR reaction, standard curves for each primer pairs were constructed using 10-fold serial dilutions of plasmid DNA. Melt curves were also generated for each products to confirm the purity of the amplicon. The R^2 coefficient was > 0.990, with primer efficiency ranging from 1.972 to 2.005. The relative mRNA expression level of the target gene was determined using the housekeeping gene elongation factor 1 α (EF-1α) as an internal reference using the $2^{-\Delta\Delta CT}$ method [35]. Each sample was run in triplicate. The statistical *P*-values were calculated by using one-way analysis of variance (one-way ANOVA) followed by Duncan's multiple comparison test. Differences were considered to be statistically significant at $P < 0.05$.

2.5. Transfection and reporter gene assays

The 5′ flanking region of AjIFN2 and AjIFN4 was amplified using primer sets contained an *Nhe* I restriction site in the forward primer and *Bam*H I site in the reverse primer (Table 1). Amplification products were gel purified and ligated into pGL3-basic (Promega). All recombinant plasmids were confirmed by DNA sequencing. EPC cells were seeded to 90% confluency in 24-well plates (1×10^6 cells/well) prior to transfection. Cells were transfected with 10 ng pRL-TK Renilla luciferase internal control vector (Promega), and 100 ng AjIFN2-pro or AjIFN4-pro, respectively. 24 h afterwards, cells were mock transfected or transfected with 1 μg/ml Poly I:C for an additional 24 h. Cells were then harvested for luminescent luciferase analysis measured with commercial reagents following the manufacturer's instruction. (Promega).

For induction assay, the coding region of AjRIG-Ib or AjRIG-Ibv was cloned into the pcDNA3.1/myc-His(+)A vector (Invitrogen) between the *Eco*R V and *Bam*H I sites, respectively. EPC cells (1×10^6 cells/well) seeded overnight in 24-well plates were cotransfected with various plasmids (pRL-TK, AjIFN2-pro or AjIFN4-pro, pcDNA3.1 or AjRIG-Ib/AjRIG-Ibv-pcDNA3.1 constructs) at a ratio of 1 : 10: 10 respectively. Empty vector DNA (pcDNA3.1) was used to keep the total amount of transfected DNA constant. Twenty-four hours after transfection, cells were lysed and assayed for reporter activity. Results are expressed as fold change over empty vector (pcDNA3.1) control. Data shown are mean ± SD from three separate experiments, each performed in triplicate.

2.6. Subcellular distribution

Expression plasmids were constructed by inserting the ORF of AjRIG-Ib or AjRIG-Ibv into p3xFLAG-CMV between *Eco*R V and *Bam*H I sites, respectively. HEK293 cells were seeded onto coverslips in 24-well plates 1 d before transfection. Cells were transfected with recombinant plasmid, AjRIG-Ib-Flag and AjRIG-Ibv-Flag or the empty control plasmids, respectively, for 24 h using Liposomes (Lip3000, ThermoFisher). Cells were then incubated with DiO for 30 min and washed three time with PBS. Afterwards, cells were fixed with 4% paraformaldehyde (PFA) for 10 min at room temperature, followed by permeabilization with 0.25% Triton X-100 in PBS for 1 h and blocked with 5% (v/v) goat serum at 37 °C for 1 h. After being washed three times with PBS, fixed cells on the coverslips were incubated with mouse monoclonal antibody against FLAG (at a dilution of 1 : 40, 66008-2-Ig, Proteintech) followed by incubation with CoraLite594 – conjugated Goat Anti-Mouse IgG (at a dilution of 1 : 200, SA00013-3, Proteintech). Cells were stained with DAPI (100 ng/ml). Images were taken using a laser scanning confocal microscope (Leica TCS SP8).

3. Results

3.1. Cloning and sequence characterization of AjRIG-Ib and AjRIG-Ibv

Two partial sequences encoding RIG-I genes were retrieved from Japanese eel draft genome using the BLAST algorithm, and the scaffold BEWY01000003.1 was found to contain the already published sequence of RIG-I [30]. The scaffold BEWY01000009.1 was found to contain a putative RIG-I gene, named here as AjRIG-Ib, that has never been characterized previously. Specific primers were designed to obtain the complete coding sequence.

The AjRIG-Ib cDNA (submitted to GenBank as MK838769) consists of 4448 nucleotides with a 2823 bp open reading frame encoding a 940-aa protein. Sequence comparison shows that AjRIG-Ib shares low similarity (39%) with previously reported eel RIG-I (GenBank accession No. KT156978). Through the alignment of AjRIG-Ib cDNA sequence against eel genomic sequence (GenBank accession No. GCA_003597225.1), we found that the AjRIG-Ib gene consists of 18 exons (Fig. 1), of which, exons 1–4 encode the two tandem N-terminal caspase activation and recruitment domains (CARDs), and exons 6–8 and the first 21 nucleotide of the ninth exon encode a DExD/H box helicase domain (DEAD). The last 66 nucleotides of the seventeenth exon and eighteenth exon encode C-terminal domain (CTD) of RIG-I (Fig. 1). In addition, we identified an alternative splicing variant of eel

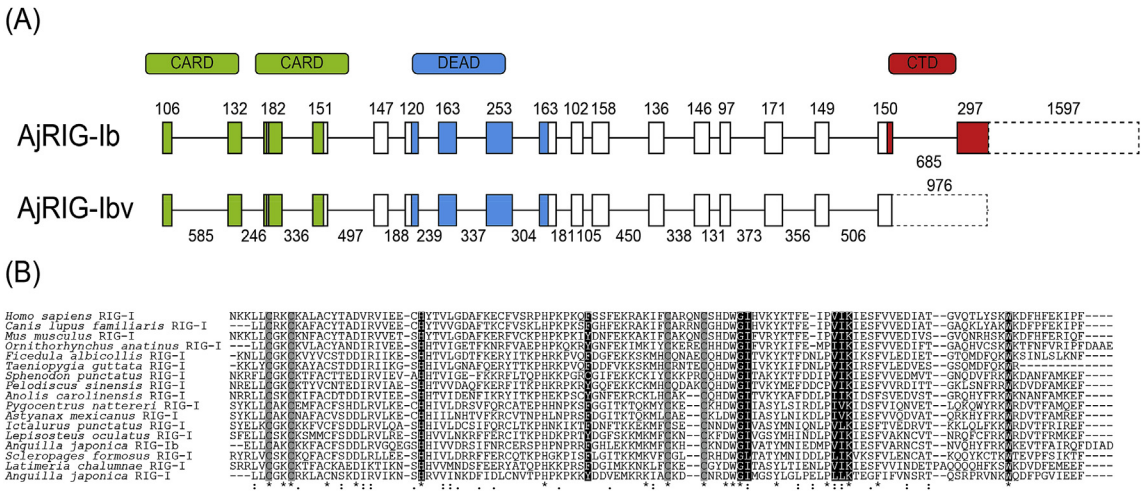

Fig. 1. Gene structure and orthologous sequence alignment. (A) Diagram of the gene structure and length (in base pairs; bp) of AjRIG-Ib and AjRIG-Ibv. CARD (green), DEAD domains (blue) and C-terminal domain (red) are represented. (B) Sequence conservation of C-terminal domain in RIG-I protein sequences. Alignments were carried out using the program ClustalX. Amino acids relative to Zn^{2+}-binding motifs are shaded with grey, dsRNA binding sites are shaded with black. (For interpretation of the references to colour in this figure legend, the reader is referred to the Web version of this article.)

RIG-I (AjRIG-Ibv) retaining intron 17 with the inclusion of a premature stop codon (submitted to GenBank as MK838770). Therefore, a truncated protein was predicted, which lacks the entire C-terminal domain (Fig. 1). In silico analysis revealed the presence of two conserved Zn^{2+}-binding motifs in the CTD of AjRIG-Ib. The first Zn^{2+}-binding motif (Cys-x-x-Cys) was highly conserved from teleost to mammals, while the second Zn^{2+}-binding motif differed from that of amniotes (except *Anolis carolinensis*), in which two conserved cysteines are separated by four aa residues (CxxxxC) (Fig. 1).

Phylogenetic trees including RIG-I, LGP2 and MDA5 in vertebrates were constructed by using both neighbor-joining and maximum likelihood reconstruction methods. The results obtained by NJ and ML were comparable, which exhibit a topology of the form [(LGP2) (MDA5)] (RIG-I) (Fig. 2 and Supplementary Fig. S1). Meanwhile, the AjRIG-Ib and AjRIG-Ibv were clustered with teleost RIG-I clade and showed the closest relationship to the RIG-I of Osteoglossiformes species (Fig. 2).

3.2. Gene expression of AjRIG-Ib and AjRIG-Ibv

Gene expression analysis showed that AjRIG-Ib was expressed in all seven tested organs/tissues (i. e. liver, intestine, head kidney, middle kidney, skin, spleen and gill) examined in all the fish, with higher levels in gill and spleen, and lower levels in intestine and liver. Despite the differences in the basal expression, AjRIG-Ibv was detectable in all tissues/organs examined. The ratio between AjRIG-Ib and AjRIG-Ibv varies in different tissues/organs with highest ratio observed in gill, followed by in spleen, skin, intestine and middle kidney, being about 36.0, 10.3, 5.3, 5.2 and 5.0 folds, respectively (Fig. 3).

To investigate the potential role of AjRIG-Ib and AjRIG-Ibv in antiviral response, their expression profile in tissues/organs of Poly I:C injected eels was investigated. As shown in Fig. 4, the expression level of AjRIG-Ib increased significantly at almost all the measured timepoints and in all tissues/organs, except in liver and skin at 8 hpi and gill at 72 hpi. The peak expression level of AjRIG-Ib was observed at 16 hpi, where an approximately 478, 236, 248, 485, 216 and 266-fold greater amount of transcripts was seen in head kidney, spleen, liver, skin, gill, and intestine respectively. Compared to AjRIG-Ib, Poly I:C-induced AjRIG-Ibv expression appeared more rapid and robust, with a 141.8-fold increase in head kidney, 112.6-fold in spleen, 60.7-fold in liver, 101.1-fold in skin, 131.5-fold in gill and 68.6-fold in intestine at 8 hpi, respectively.

3.3. Subcelluar localization of AjRIG-Ib and AjRIG-Ibv

To determine the intracellular localization of AjRIG-Ib and AjRIG-Ibv, immunofluorescence assays were employed. HEK293T cells were transfected with AjRIG-Ib-Flag and AjRIG-Ibv-Flag respectively. As shown in Fig. 5, the staining of AjRIG-Ib and AjRIG-Ibv was mainly concentrated in the cytoplasm of cells.

3.4. IFN inducibility of AjRIG-Ib and AjRIG-Ibv

To assess the role of AjRIG-Ib and AjRIG-Ibv in the activation of type I IFN promoter, we cloned the promoter region of AjIFN2 and AjIFN4 and fused them to the luciferase open reading frame. The luciferase measurement was performed to test whether the AjIFN promoters constructed in this study can response to Poly I:C stimulation. EPC cells were transfected with AjIFN2 or AjIFN4 promoter reporter, or pGL3-basic empty vector for 24 h, separately, followed by transfection with Poly I:C. The transfection of Poly I:C increased the promoter activity of AjIFN2 and AjIFN4, up to19.5 and 1.9 folds, respectively.

EPC cells were then co-transfected with the AjIFN2 or AjIFN4 promoter reporter and with either AjRIG-Ib-pcDNA3.1 or AjRIG-Ibv-pcDNA3.1. As shown in Fig. 6, the overexpression of AjRIG-Ib in cells resulted in a 2.7 and 3.2-fold up-regulation of AjIFN2 and AjIFN4 promoter luciferase activity compared with control cells transfected with the empty pCDNA3.1 plasmid, respectively. The overexpression of AjRIG-Ibv resulted in the induction of AjIFN2 and AjIFN4 promoter activity with the up-regulation of 2.4 and 3.8 folds, respectively.

4. Discussion

Previously, an isoform of RIG-I gene was reported in Japanese eel, which exhibited protein structure similar to that of their mammalian counterparts [30]. In the present study, we have characterized a novel isoform of RIG-I and its splicing variant in Japanese eel, which shared low sequence similarity (39%) to that reported by Feng and coworkers [30]. Meanwhile, blast search against eel genome shows that the two RIG-I genes are located on different scaffolds, indicating possibly that they may be derived from an individual duplication event or from genome wide duplication in eels. However, additional data, such as the discovery of RIG-I-like isoforms in other teleost fish are required to support this speculation.

Studies in mammals have demonstrated that the two N-terminal CARDs of RIG-I are responsible for the interaction of MAVS, leading to

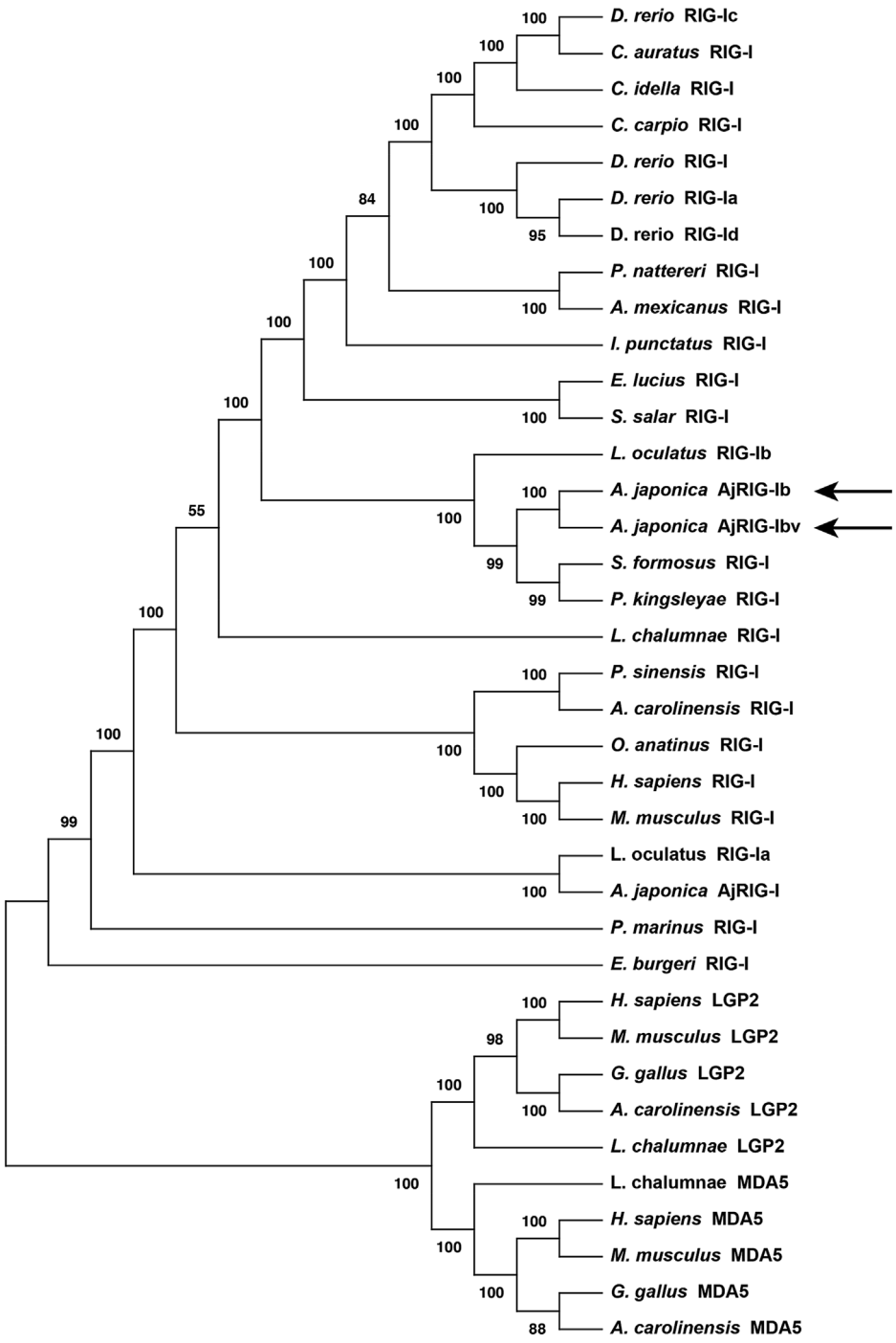

Fig. 2. A neighbor-joining tree showing the relationship of the RLR proteins in vertebrates. Bootstrap values (N = 10 000) were given at the node of each branch. AjRIG-Ib and AjRIG-Ibv are indicated with arrows.

the production of type I IFNs [18,36,37]. The helicase domain and C-terminal domain (CTD) together, function as an integrated RNA binding unit, but it is the CTD that specifically binds viral RNA or ssRNA viral genomes in a 5′-triphosphate-dependent manner [12,38,39]. Co-operative ATP and dsRNA binding to the helicase domain induces a conformational switch, which in turns releases the CARDs for ubiquitination and downstream signaling via MAVS [40]. Comparatively, fish RIG-I protein possesses similar structural and functional characteristics as those seen in their mammalian counterparts [41]. For example, eight conserved residues (845H, 868F, 887G, 888I, 900V, 901I, 902K, 922W) were identified in the CTD of AjRIG-Ib, which may be involved in dsRNA binding. In addition, two CxxC motifs in the CTD of AjRIG-Ib were implicated in Zn^{2+} binding. In mammals, mutation of zinc-coordinating cysteine residues can lead to the abrogation of response to Vesicular stomatitis virus infection [39]. These findings raise the possibility that the CTD of AjRIG-Ib is involved in viral RNA sensing, as its mammalian counterparts.

In resting cells, the CTD of RIG-I is phosphorylated by CK2α at aa Thr770 and Ser854 to 855, which leads to the interaction of CTD and CARDs to form a closed, inactivated conformation [42]. Upon viral infection, CTD is dephosphorylated, resulting in disassociation of intermolecular interaction, thus activating RIG-I [43]. CK2α is the catalytic subunit of protein kinase CK2, an acidophilic Ser/Thr protein kinase with the specific recognition motif that is characterized with either

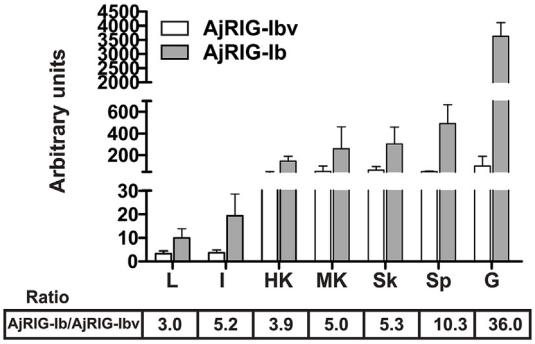

Ratio							
AjRIG-Ib/AjRIG-Ibv	3.0	5.2	3.9	5.0	5.3	10.3	36.0

Fig. 3. Relative gene expression of AjRIG-Ib and AjRIG-Ibv in tissues/organs from healthy Japanese eel. The expression level for each transcript was normalized to house-keeping gene (Elongation factor 1 α, EF-1α) expression and calculated as arbitrary units. L, I, HK, MK, Sk, Sp, G representing liver, intestine, head kidney, middle kidney, skin, spleen and gill, respectively. For comparison, one arbitrary unit was equal to the transcript amount of AjRIG-Ibv in the liver, where the lowest level was observed. The ratio of expression level of AjRIG-Ib and AjRIG-Ibv is shown below the graphs. The results represent the mean ± SD of ten fish.

glutamic acid (E) or aspartic acid residues (D) near the phosphorylation site (S/T-X-X-D/E/pS/pY) [44–46]. Motif scan analysis revealed the lack of canonical CK2 consensus in the CTD of AjRIG-I, and Thr770 is substituted by glutamine (Q), Ser854 and 855 are substituted by glicine (G) and histidine (H) in AjRIG-Ib, respectively. However, studies in mammals showed that the serine 392 site of p53 was efficiently phosphorylated by CK2, whereas the adjacent sequence does not match the CK2 recognition consensus [47,48]. Keeping this in view, we cannot exclude the possibility of CK2-dependent phosphorylation of RIG-I in teleost.

It is worthy to note that the variant, AjRIG-Ibv, encompassed tandem CARDs and a helicase domain, but was devoid of the CTD. Alternative splicing is increasingly recognized as one of important mechanisms for gene regulation that allows individual genes to express multiple mRNAs, yielding proteins with different or even antagonistic functions [49,50]. In mammals, a splice variant of RIG-I (RIG-I SV), carrying a short deletion (amino acids 36–80) within CARD1, is significantly induced upon IFN-β treatment or Sendai virus (SeV)-infection [51]. RIG-I SV acts as inhibitor of RIG-I signal transduction by forming a hetero-oligomer with full-length RIG-I, thus preventing RIG-I-MAVS interaction [51]. In zebrafish, four different splicing variants of RIG-I have been characterized [28,31,41]. The canonical form, termed as RIG-Ib, shares primary structural similarity and IFN inducibility with mammalian RIG-I. Meanwhile, RIG-Ia encodes a protein with 38 aa insertion in the second CARD domain of RIG-Ib. RIG-Ic encodes a protein with the deletion of 3 aa at position 189 (taking zebrafish RIG-Ib as a reference), while RIG-Id encodes a protein with 2 aa deletion at position 189 and 3 aa insertion at position 597 [28,31]. These variants may be resulted from alterations in the splice donor or acceptor sites for the exons without altering the reading frame or overall protein

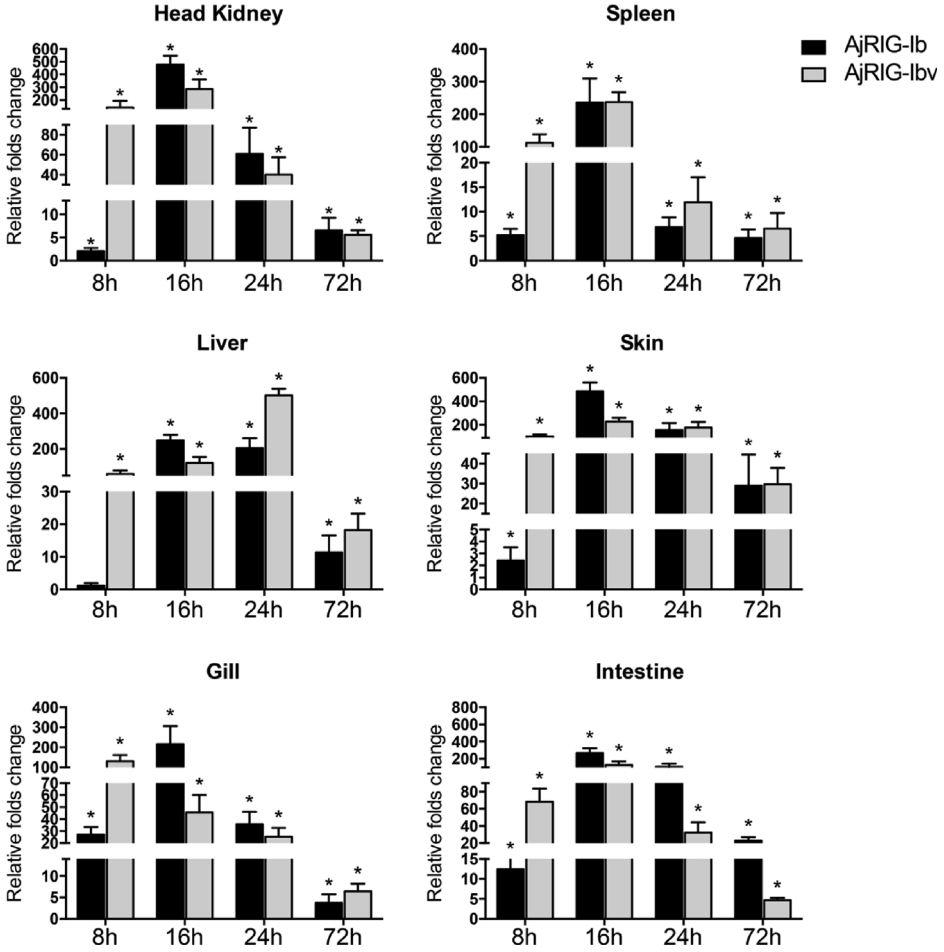

Fig. 4. QPCR analysis of AjRIG-Ib and AjRIG-Ibv expression in response to Poly I:C stimulation. Tissues/organs, including head kidney, spleen, liver, skin, gill intestine, were collected at different time points after Poly I:C challenge, and results were presented as fold-change as compared to the control group (PBS injection). AjRIG-Ib and AjRIG-Ibv transcripts were normalized to the expression level of the housekeeping gene (EF-1a) by the $2^{-\Delta\Delta CT}$ method. Data are expressed as mean ± SD (n = 6). Significant difference was indicated by asterisks, *: $P < 0.05$.

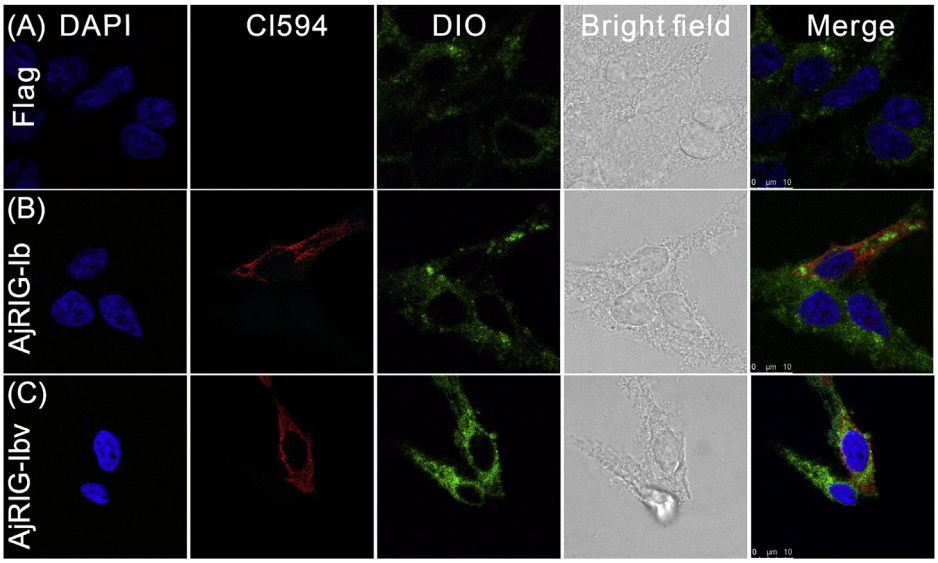

Fig. 5. Confocal microscopic analysis of the cellular distribution of AjRIG-Ib and AjRIG-Ibv. HEK293T cells were transfected with empty plasmid p3xFLAG (Line A) and AjRIG-Ib-flag (Line B), and AjRIG-Ibv-flag (Line C), respectively, and then fixed and stained. Cell nuclei were stained with blue using DAPI, and the membranes and cytoplasm were stained with green using DIO. Secondary antibody (CoraLite594 – conjugated Goat Anti-Mouse IgG) stains AjRIG-Ib and AjRIG-Ibv, respectively (red). (For interpretation of the references to colour in this figure legend, the reader is referred to the Web version of this article.)

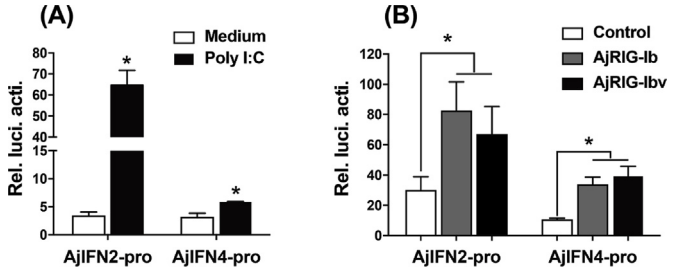

Fig. 6. Effect of AjRIG-Ib or AjRIG-Ibv on the expression of luciferase from the eel IFN promoter constructs. Luciferase activity was measured in cells co-transfected with one of following vector combinations: (A) AjIFN2 or AjIFN4 constructs and pRL-TK, followed by Poly I:C transfection. (B) AjRIG-Ib-flag or AjRIG-Ibv-flag and each AjIFN promoters, respectively. Data are mean ± SD. Experiments were repeated three times. Asterisks (*) above each bars indicate significant difference ($P < 0.05$) compared with control.

structure. Instead, AjRIG-Ibv identified in this study is an intron-retained transcript variant, and a new kind spliced isoform previously unreported. Studies in mammals have shown that mutants of RIG-I proteins lacking inhibitory domain are typically constitutively activated, leading to enhanced IFN production in RIG-I-deficient human hepatoma cell line (Huh 7.5) [43,52]. Cells transfected with mutants lacking CTD exhibited a powerful antiviral effect against grass carp reovirus, and the relative expression of downstream genes, for example MAVS, IFN and Mx, was highly induced [53]. Our results showed that the expression of AjRIG-Ibv increased rapidly in all examined tissues/organs after Poly I:C stimulation, being as early as 8 hpi, indicating that AjRIG-Ibv plays an important role in early defense against viral infection. However, further research is required to clarify its precise function.

In conclusion, two transcript variants of RIG-I gene were identified in Japanese eel. AjRIG-Ib contains a typical domain organization, with two CARDs followed by a helicase domain and a C-terminal domain, but AjRIG-Ibv lacks C-terminal domain. The two RIG-I isoforms shared similar cellular distribution and IFN inducibility. The expression of AjRIG-Ibv was rapidly induced at the early stage of Poly I:C stimulation, while AjRIG-Ib was significantly up-regulated in late stage. Therefore, it is likely that the two RIG-I variants may play cooperative and complementary roles in antiviral immunity of fish.

Acknowledgements

The research was supported by the Natural Science Foundation of Fujian Province (No. 2016J06008), China Agricultural Research System (CARS-46) and the National Natural Science Foundation of China (Grant No. 31402329).

Appendix A. Supplementary data

Supplementary data to this article can be found online at https://doi.org/10.1016/j.fsi.2019.09.037.

References

[1] C.A. Janeway Jr., R. Medzhitov, Innate immune recognition, Annu. Rev. Immunol. 20 (2002) 197–216.
[2] R. Medzhitov, Toll-like receptors and innate immunity, Nat. Rev. Immunol. 1 (2001) 135–145.
[3] S. Akira, S. Uematsu, O. Takeuchi, Pathogen recognition and innate immunity, Cell 124 (2006) 783–801.
[4] M. Yoneyama, M. Kikuchi, T. Natsukawa, N. Shinobu, T. Imaizumi, M. Miyagishi, et al., The RNA helicase RIG-I has an essential function in double-stranded RNA-induced innate antiviral responses, Nat. Immunol. 5 (2004) 730–737.
[5] T. Kawai, S. Akira, The role of pattern-recognition receptors in innate immunity: update on Toll-like receptors, Nat. Immunol. 11 (2010) 373–384.
[6] Y.M. Loo, M. Gale Jr., Immune signaling by RIG-I-like receptors, Immunity 34 (2011) 680–692.
[7] K.R. Rodriguez, A.M. Bruns, C.M. Horvath, MDA5 and LGP2: accomplices and antagonists of antiviral signal transduction, J. Virol. 88 (2014) 8194–8200.
[8] Y.K. Chan, M.U. Gack, RIG-I-like receptor regulation in virus infection and immunity, Curr. Opin. Virol. 12 (2015) 7–14.
[9] X. Zhang, C. Wang, L.B. Schook, R.J. Hawken, M.S. Rutherford, An RNA helicase, RHIV-1, induced by porcine reproductive and respiratory syndrome virus (PRRSV) is mapped on porcine chromosome 10q13, Microb. Pathog. 28 (2000) 267–278.
[10] H. Kato, S. Sato, M. Yoneyama, M. Yamamoto, S. Uematsu, K. Matsui, et al., Cell type-specific involvement of RIG-I in antiviral response, Immunity 23 (2005) 19–28.
[11] M. Yoneyama, M. Kikuchi, K. Matsumoto, T. Imaizumi, M. Miyagishi, K. Taira, et al., Shared and unique functions of the DExD/H-box helicases RIG-I, MDA5, and LGP2 in antiviral innate immunity, J. Immunol. 175 (2005) 2851–2858.
[12] V. Hornung, J. Ellegast, S. Kim, K. Brzozka, A. Jung, H. Kato, et al., 5'-Triphosphate RNA is the ligand for RIG-I, Science 314 (2006) 994–997.
[13] H. Kato, O. Takeuchi, S. Sato, M. Yoneyama, M. Yamamoto, K. Matsui, et al., Differential roles of MDA5 and RIG-I helicases in the recognition of RNA viruses, Nature 441 (2006) 101–105.
[14] Y.M. Loo, J. Fornek, N. Crochet, G. Bajwa, O. Perwitasari, L. Martinez-Sobrido, et al., Distinct RIG-I and MDA5 signaling by RNA viruses in innate immunity, J. Virol. 82 (2008) 335–345.
[15] M. Habjan, I. Andersson, J. Klingstrom, M. Schumann, A. Martin, P. Zimmermann, et al., Processing of genome 5' termini as a strategy of negative-strand RNA viruses to avoid RIG-I-dependent interferon induction, PLoS One 3 (2008) e2032.
[16] S. Zhou, A.M. Cerny, A. Zacharia, K.A. Fitzgerald, E.A. Kurt-Jones, R.W. Finberg, Induction and inhibition of type I interferon responses by distinct components of

lymphocytic choriomeningitis virus, J. Virol. 84 (2010) 9452–9462.
[17] B. Wu, S. Hur, How RIG-I like receptors activate MAVS, Curr. Opin. Virol. 12 (2015) 91–98.
[18] T. Kawai, K. Takahashi, S. Sato, C. Coban, H. Kumar, H. Kato, et al., IPS-1, an adaptor triggering RIG-I- and Mda5-mediated type I interferon induction, Nat. Immunol. 6 (2005) 981–988.
[19] H. Kato, K. Takahasi, T. Fujita, RIG-I-like receptors: cytoplasmic sensors for non-self RNA, Immunol. Rev. 243 (2011) 91–98.
[20] C. Stein, M. Caccamo, G. Laird, M. Leptin, Conservation and divergence of gene families encoding components of innate immune response systems in zebrafish, Genome Biol. 8 (2007) R251.
[21] Y. Palti, Toll-like receptors in bony fish: from genomics to function, Dev. Comp. Immunol. 35 (2011) 1263–1272.
[22] J. Zou, M. Chang, P. Nie, C.J. Secombes, Origin and evolution of the RIG-I like RNA helicase gene family, BMC Evol. Biol. 9 (2009) 85.
[23] S. Biacchesi, M. LeBerre, A. Lamoureux, Y. Louise, E. Lauret, P. Boudinot, et al., Mitochondrial antiviral signaling protein plays a major role in induction of the fish innate immune response against RNA and DNA viruses, J. Virol. 83 (2009) 7815–7827.
[24] F. Sun, Y.B. Zhang, T.K. Liu, J. Shi, B. Wang, J.F. Gui, Fish MITA serves as a mediator for distinct fish IFN gene activation dependent on IRF3 or IRF7, J. Immunol. 187 (2011) 2531–2539.
[25] C. Yang, J. Su, T. Huang, R. Zhang, L. Peng, Identification of a retinoic acid-inducible gene I from grass carp (*Ctenopharyngodon idella*) and expression analysis in vivo and in vitro, Fish Shellfish Immunol. 30 (2011) 936–943.
[26] H. Feng, H. Liu, R. Kong, L. Wang, Y. Wang, W. Hu, et al., Expression profiles of carp IRF-3/-7 correlate with the up-regulation of RIG-I/MAVS/TRAF3/TBK1, four pivotal molecules in RIG-I signaling pathway, Fish Shellfish Immunol. 30 (2011) 1159–1169.
[27] K.V. Rajendran, J. Zhang, S. Liu, E. Peatman, H. Kucuktas, X. Wang, et al., Pathogen recognition receptors in channel catfish: II. Identification, phylogeny and expression of retinoic acid-inducible gene I (RIG-I)-like receptors (RLRs), Dev. Comp. Immunol. 37 (2012) 381–389.
[28] P.F. Zou, M.X. Chang, Y. Li, S. Huan Zhang, J.P. Fu, S.N. Chen, et al., Higher antiviral response of RIG-I through enhancing RIG-I/MAVS-mediated signaling by its long insertion variant in zebrafish, Fish Shellfish Immunol. 43 (2015) 13–24.
[29] L. Nie, Y.S. Zhang, W.R. Dong, L.X. Xiang, J.Z. Shao, Involvement of zebrafish RIG-I in NF-kappaB and IFN signaling pathways: insights into functional conservation of RIG-I in antiviral innate immunity, Dev. Comp. Immunol. 48 (2015) 95–101.
[30] J. Feng, S. Guo, P. Lin, Y. Wang, Z. Zhang, L. Yu, Identification of a retinoic acid-inducible gene I from Japanese eel (*Anguilla japonica*) and expression analysis in vivo and in vitro, Fish Shellfish Immunol. 55 (2016) 249–256.
[31] M.X. Chang, J. Zhang, Alternative pre-mRNA splicing in mammals and teleost fish: a effective strategy for the regulation of immune responses against pathogen infection, Int. J. Mol. Sci. 18 (2017) 1530.
[32] J.J. Campanella, L. Bitincka, J. Smalley, MatGAT: an application that generates similarity/identity matrices using protein or DNA sequences, BMC Bioinf. 4 (2003) 29.
[33] A. Stamatakis, RAxML version 8: a tool for phylogenetic analysis and post-analysis of large phylogenies, Bioinformatics 30 (2014) 1312–1313.
[34] D. Darriba, G.L. Taboada, R. Doallo, D. Posada, ProtTest 3: fast selection of best-fit models of protein evolution, Bioinformatics 27 (2011) 1164–1165.
[35] K.J. Livak, T.D. Schmittgen, Analysis of relative gene expression data using real-time quantitative PCR and the 2(-Delta Delta C(T)) Method, Methods 25 (2001) 402–408.
[36] E. Meylan, J. Tschopp, M. Karin, Intracellular pattern recognition receptors in the host response, Nature 442 (2006) 39–44.
[37] J.W. Schoggins, S.J. Wilson, M. Panis, M.Y. Murphy, C.T. Jones, P. Bieniasz, et al., A diverse range of gene products are effectors of the type I interferon antiviral response, Nature 472 (2011) 481–485.
[38] A. Pichlmair, O. Schulz, C.P. Tan, T.I. Naslund, P. Liljestrom, F. Weber, et al., RIG-I-mediated antiviral responses to single-stranded RNA bearing 5'-phosphates, Science 314 (2006) 997–1001.
[39] S. Cui, K. Eisenacher, A. Kirchhofer, K. Brzozka, A. Lammens, K. Lammens, et al., The C-terminal regulatory domain is the RNA 5'-triphosphate sensor of RIG-I, Mol. Cell 29 (2008) 169–179.
[40] E. Kowalinski, T. Lunardi, A.A. McCarthy, J. Louber, J. Brunel, B. Grigorov, et al., Structural basis for the activation of innate immune pattern-recognition receptor RIG-I by viral RNA, Cell 147 (2011) 423–435.
[41] S.N. Chen, P.F. Zou, P. Nie, Retinoic acid-inducible gene I (RIG-I)-like receptors (RLRs) in fish: current knowledge and future perspectives, Immunology 151 (2017) 16–25.
[42] Z. Sun, H. Ren, Y. Liu, J.L. Teeling, J. Gu, Phosphorylation of RIG-I by casein kinase II inhibits its antiviral response, J. Virol. 85 (2011) 1036–1047.
[43] T. Saito, R. Hirai, Y.M. Loo, D. Owen, C.L. Johnson, S.C. Sinha, et al., Regulation of innate antiviral defenses through a shared repressor domain in RIG-I and LGP2, Proc. Natl. Acad. Sci. U.S.A. 104 (2007) 582–587.
[44] D.W. Litchfield, A. Arendt, F.J. Lozeman, E.G. Krebs, P.A. Hargrave, K. Palczewski, Synthetic phosphopeptides are substrates for casein kinase II, FEBS Lett. 261 (1990) 117–120.
[45] O. Marin, F. Meggio, G. Draetta, L.A. Pinna, The consensus sequences for cdc2 kinase and for casein kinase-2 are mutually incompatible. A study with peptides derived from the beta-subunit of casein kinase-2, FEBS Lett. 301 (1992) 111–114.
[46] N. St-Denis, M. Gabriel, J.P. Turowec, G.B. Gloor, S.S. Li, A.C. Gingras, et al., Systematic investigation of hierarchical phosphorylation by protein kinase CK2, J. Proteom. 118 (2015) 49–62.
[47] D.W. Meek, S. Simon, U. Kikkawa, W. Eckhart, The p53 tumour suppressor protein is phosphorylated at serine 389 by casein kinase II, EMBO J. 9 (1990) 3253–3260.
[48] F. Meggio, O. Marin, L.A. Pinna, Substrate specificity of protein kinase CK2, Cell. Mol. Biol. Res. 40 (1994) 401–409.
[49] B. Modrek, C. Lee, A genomic view of alternative splicing, Nat. Genet. 30 (2002) 13–19.
[50] F.E. Baralle, J. Giudice, Alternative splicing as a regulator of development and tissue identity, Nat. Rev. Mol. Cell Biol. 18 (2017) 437–451.
[51] M.U. Gack, A. Kirchhofer, Y.C. Shin, K.S. Inn, C. Liang, S. Cui, et al., Roles of RIG-I N-terminal tandem CARD and splice variant in TRIM25-mediated antiviral signal transduction, Proc. Natl. Acad. Sci. U.S.A. 105 (2008) 16743–16748.
[52] R. Sumpter Jr., Y.M. Loo, E. Foy, K. Li, M. Yoneyama, T. Fujita, et al., Regulating intracellular antiviral defense and permissiveness to hepatitis C virus RNA replication through a cellular RNA helicase, RIG-I, J. Virol. 79 (2005) 2689–2699.
[53] L. Chen, J. Su, C. Yang, L. Peng, Q. Wan, L. Wang, Functional characterizations of RIG-I to GCRV and viral/bacterial PAMPs in grass carp *Ctenopharyngodon idella*, PLoS One 7 (2012) e42182.